GEOPHYSICS, VOL. 56, NO. 12 (DECEMBER 1991); P. 2139–2147, 11 FIGS., 1 TABLE.

Hysteresis in the electrical resistivity of partially saturated sandstones

Rosemary Knight*

ABSTRACT

Laboratory measurements of the resistivity of three sandstone samples collected during imbibition (increasing Sw) and drainage (decreasing Sw) show pronounced hysteresis in resistivity throughout much of the saturation range. The variation in resistivity can be related to changes in pore-scale fluid distribution caused by changes in saturation history. The form of the hysteresis is such that resistivity measured during imbibition is consistently less than that measured, at the same saturation, during drainage. This can be attributed to the presence of conduction at the air/water interface in partially saturated samples; an effect that is enhanced by fluid geometries associated with the imbibition process. The results of this study suggest that the dependence of geophysical data on saturation history should be considered when interpreting data from the unsaturated zone.

INTRODUCTION

There is rapidly growing interest in the application of geophysical techniques to hydrogeologic problems. One particular area of interest is the use of surface or borehole electrical resistivity measurements to determine or monitor water content and water quality in the unsaturated zone. In the interpretation of electrical resistivity data from the unsaturated zone the form of variation of resistivity with water content must first be characterized. While it is quite clear that the electrical resistivity (ρ) of a material is related to water content, the laboratory study described in this paper reveals that this is not a simple relationship in partially saturated geological materials.

Hydrogeologic studies of the unsaturated zone have established that the relationships between hydraulic conductivity, fluid pressure, and water content are hysteretic. The existence of hysteresis can be attributed, at least in part, to the fact that changes in the saturation process (i.e., wetting versus drying) cause changes in the pore-scale fluid distribution. In the dependence of hydraulic conductivity on water content, for example, numerous distinct curves can be obtained during sequences of wetting and drying that characterize the geological material of interest.

It is becoming increasingly apparent that measured geophysical properties of geological materials are also strongly affected by the details of the pore-scale fluid distribution. Laboratory measurements of the dielectric constant (Knight and Nur, 1987a), electrical resistivity (Longeron et al., 1989), elastic wave velocities (Knight and Nolen-Hoeksema, 1990), and elastic wave attenuation (Bourbie and Zinszner, 1984) all exhibit variations in the dependence of the measured property on the level of water saturation that are caused by changes in pore-scale fluid distribution. In these laboratory experiments the changes in fluid distribution were caused by changes in saturation technique. Near the surface of the earth, the unsaturated zone experiences many natural changes in "saturation technique." A complicated saturation history of repeated cycles of wetting and drying can lead to high variability in pore-scale fluid distribution. Thus, in order to accurately interpret geophysical data from the unsaturated zone, the form of dependence of geophysical data on fluid distribution needs to be more fully understood.

Longeron et al. (1989) found hysteresis in the electrical resistivity of sandstone and limestone samples when saturation, with a mixture of oil and brine, was varied by imbibition and drainage. Imbibition is the increase of water saturation in a water-wet sample by the displacement of a nonwetting fluid by water; drainage is the decrease of water saturation in a water-wet sample by the displacement of water by a nonwetting fluid. The purpose of this study was to investigate such an effect in samples saturated with air and water in order to assess the implications for interpreting resistivity data from the unsaturated zone. In this paper I present the results of a laboratory study of the electrical resistivity of three sandstones measured during repeated imbibition/drainage cycles. These results clearly show that

Manuscript received by the Editor March 19, 1991; revised manuscript received July 30, 1991.
*Department of Geological Sciences, University of British Columbia, Vancouver, B.C., Canada V6T 1Z4.

saturation-related hysteresis exists in electrical properties as it does in hydraulic properties. While this initially appears only to complicate the interpretation of electrical measurements made in the unsaturated zone, it also introduces the intriguing possibility that information about in situ pore-scale fluid distributions can be extracted from geophysical data.

SAMPLE DESCRIPTION AND EXPERIMENTAL PROCEDURE

The samples used in this study are three sandstones, described in Table 1. Samples CH58-79, CH61-79 are sandstones from the Spirit River Formation in the Alberta Basin. These samples have very low porosity and permeability with a considerable amount of carbonate cement and a moderately high clay content in the form of argillaceous lithics and as a clay cement. Berea 100 sandstone is a quarried high porosity sandstone, best described as a sublitharenite; the clay fraction is predominantly kaolinite. The permeabilities and petrographic descriptions in Table 1 are taken from the Stanford Rock Physics Catalogue. The permeability value for Berea 100 was determined using a steady state brine flow test; the permeabilities of CH58-79 and CH61-79 were measured using a pulse decay permeameter. The petrographic description of each sandstone is based on a 400 point count analysis of the thin section. The porosities were determined using a helium porosimeter. The surface areas, taken from Knight and Nur (1987b), were obtained from nitrogen adsorption isotherms by using the Brunauer-Emmett-Teller equation (Brunauer et al., 1938).

The laboratory resistivity measurements were made on disk-shaped samples. A two-electrode technique was used with electrodes applied by sputtering 100 nm of platinum on the two opposite flat faces of the sample disks. Data were collected in the frequency range of 60 kHz to 13 MHz; this is above the frequency range affected by polarization at the sample/electrode interface (Knight and Nur, 1987b). A Hewlett-Packard 4192A impedance analyzer was used to measure the complex admittance Y^*,

$$Y^* = G_p + iB_p$$

where G_p is the conductance and B_p is the susceptance. The electrical resistivity ρ is calculated from G_p,

$$\rho = \frac{1}{G_p}\frac{A}{t},$$

where A is the cross-sectional area of the sample and t is its thickness. Additional details of the measurement procedure and system calibration are given in Knight (1985) and Knight and Nur (1987b).

The purpose of this study was to characterize the dependence of electrical resistivity on the level of water saturation during an imbibition/drainage cycle. The level of water saturation Sw is defined as the volume fraction of the pore space filled with water, the remainder being filled with air. Imbibition data were collected by gradually increasing Sw in a dry sample through exposure to progressively higher levels of humidity. Using this technique, the maximum saturation level obtained was $Sw = 0.42$ in CH58-79; $Sw = 0.48$ in CH61-79; and $Sw = 0.06$ in Berea 100. Following this procedure, higher saturation levels were obtained by soaking the sample in a beaker of deionized water. The maximum saturation level obtained for CH58-79, CH61-79, and Berea 100 was $Sw = 0.96, 0.87$, and 0.81 respectively. The inability to reach higher saturation levels was undoubtedly due to the presence of trapped gas in the pore space. Drainage data for all samples were obtained by drying the sample through evaporation. The drying of a sample to low values of Sw was accomplished by vacuum drying and/or placing the sample in a dessicator containing the dessicant calcium sulfate.

As Sw was varied using the techniques described above, the weight of the sample was monitored to determine Sw. The planned experimental procedure was to measure electrical resistivity for changes in Sw of approximately 0.02. The time between measurements varied due to the dependence of the wetting and drying rates on the saturation levels, and sometimes it was not possible to collect data at these saturation intervals. To obtain a complete imbibition/drainage cycle required six to eight weeks for each sample. For the samples CH61-79 and Berea 100, the entire procedure was repeated twice; for CH58-79 the procedure was repeated three times.

EXPERIMENTAL RESULTS

One data set for each of the three samples is shown in Figures 1 through 3 as a plot of log ρ versus Sw. As repeated data sets were collected using the same samples, each of the data sets shown in Figures 1 through 3 will be referred to as experiment 1 for each of the samples. Figure 1 shows data collected for sample CH58-79 during an imbibition/drainage cycle; in Figure 2 are data for CH61-79; in Figure 3 are data

Table 1. Sample description

				Petrographic description (as percent of total)							
				Framework grains				Cements			
Sample	ϕ	k	S (m^2/g)	quartz	chert	feld-spar	lithics	quartz	clay	iron oxide	carbon-ates
CH58-79	.069	10.30 μD(a)	2.07	30	12	—	6	—	18	—	18
CH61-79	.070	7.18 μD(a)	2.97	38	16	1	4(b)	16	3	—	15
Berea 100	.197	84 mD	1.23	53	2	3	8	11	7(c)	—	7

ϕ = porosity; k = permeability; S = surface area. (a) In-situ conditions, (b) argillaceous, (c) clay percentage includes minor chlorite and/or sericite.

for Berea. The frequency at which these data were collected is 60 kHz. In the three samples, the dependence of log ρ on Sw is qualitatively very similar such that three regions can be defined in the data: region 1, at low Sw, which exhibits no hysteresis; region 2, at intermediate saturations, which exhibits hysteresis; and region 3 at the highest saturations which also exhibits no hysteresis.

In region 1 the resistivity of the three samples shows a large change with the addition or removal of a small amount of water. Resistivity in this region changes approximately three orders of magnitude in the three data sets. For each of the samples, there is excellent reproduceability of the data obtained during imbibition and drainage at these saturations, such that a unique relationship between ρ and Sw can be defined for each sample regardless of the saturation technique.

Region 2 is the one of greatest interest in this study, as it is clear from the data that there does not exist a unique dependence of ρ on Sw in this region. At any given value of Sw, ρ measured during imbibition is consistently less than ρ measured during drainage. The form of the hysteresis in region 2 is strikingly similar for the three samples. In the three data sets, log ρ decreases monotonically during imbibition until a critical point at midsaturations, where log ρ increases rapidly with increasing Sw over a short saturation range. For the two tight gas sandstones, CH58-79 and CH61-79, the critical saturation point is approximately Sw = 0.7; for Berea 100 the critical saturation point is approximately Sw = 0.5. An important, and very surprising observation is the fact that ρ measured during imbibition throughout much of region 2 is lower than ρ of the rock at its maximum saturated state. This is an observation that will be considered in the interpretation of the data.

At saturations above the hysteretic region, the data are somewhat scattered but show no clear hysteresis. In this region, defined as region 3, log ρ decreases gradually with increasing Sw.

The imbibition/drainage cycle was repeated three times for sample CH58-79. The data from experiment 1 and experiment 2 are shown in Figure 4 as log ρ versus Sw. To look in greater detail at the hysteretic region, regions 2 and 3 are shown as ρ versus Sw in Figure 5. It can be seen from these figures that the data in experiments 1 and 2 show very good reproduceability.

The results from the third imbibition/drainage cycle for CH58-79, referred to as experiment 3, are shown in Figure 6. The results obtained are quite different from those of the other two experiments. These data show no hysteresis in the measured resistivity. There is no obvious experimental factor that can explain this difference between experiments 1 and 2, and experiment 3.

The reproduceability of the hysteretic region was also assessed for sample CH61-79 by repeating the imbibition/drainage cycle twice. The two data sets for CH61-79, referred to as experiment 1 and experiment 2, are shown in Figure 7. While the data set collected in experiment 2 also exhibits hysteresis, these two data sets are not as closely

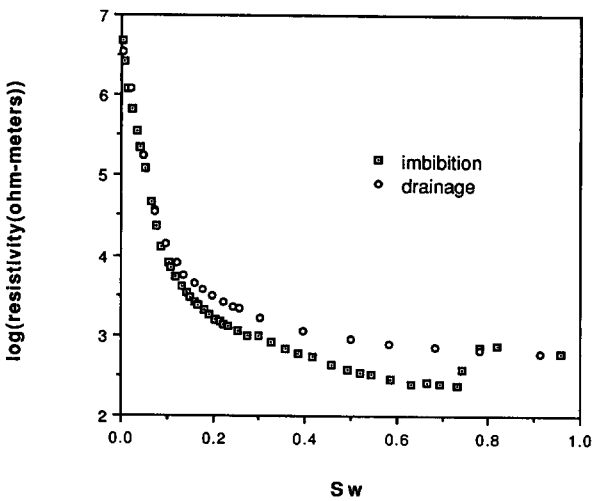

FIG. 1. Log ρ versus Sw for sample CH58-79, experiment 1; measurement frequency is 60 kHz.

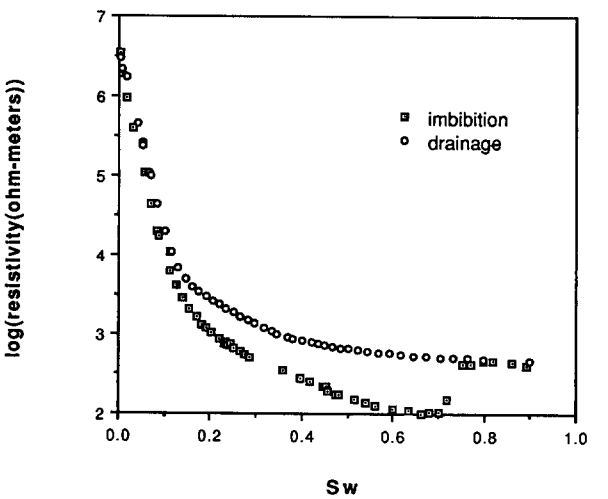

FIG. 2. Log ρ versus Sw for sample CH61-79, experiment 1; measurement frequency is 60 kHz.

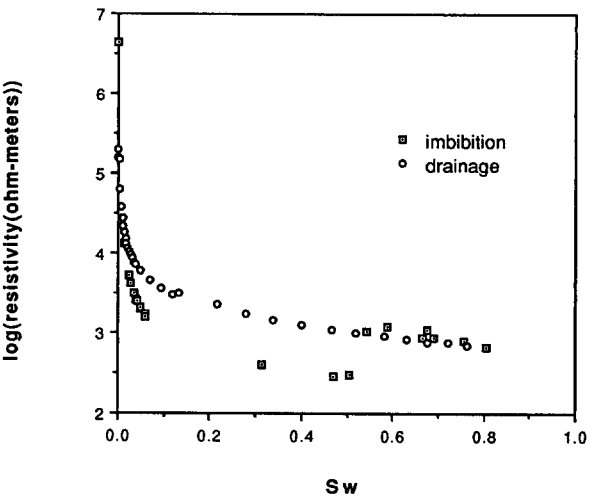

FIG. 3. Log ρ versus Sw for sample Berea 100, experiment 1; measurement frequency is 60 kHz.

matched as experiments 1 and 2 for CH58-79. The drainage data are reproduced; there is some variation in the imbibition data.

The data collected for Berea 100 in experiments 1 and 2 are shown in Figure 8. The data are somewhat sparse in the imbibition stage, but it can be seen that both data sets exhibit hysteresis between the imbibition and drainage data.

Data were collected at multiple frequencies for the three samples, usually in the frequency range of 60 kHz to 4 MHz. For CH61-79, the data in experiment 1 were collected at frequencies from 5 Hz to 13 MHz. The measured ρ of CH61-79 at several saturations, Sw = 0.07, 0.19, 0.58, 0.60, 0.92, is plotted as log ρ versus log frequency from 5 Hz to 13 MHz in Figure 9. As indicated in the figure, some of these saturations were obtained during imbibition, some during drainage. At low saturations (Sw = 0.07), the resistivity of the rock sample shows significant dispersion with log ρ decreasing with increasing frequency. At saturations in the hysteretic region, however, resistivity shows little dependence on frequency until frequencies above approximately 1 MHz. The lack of frequency dependence in the hysteretic region indicates that the magnitude of the hysteresis shown at 60 kHz for the sandstones will be observed at all frequencies in the range from 5 Hz to 1 MHz.

The results of the resistivity measurements made on the three sandstones during imbibition/drainage experiments are qualitatively very similar, with three regions that can be defined in the data sets. At low Sw, the resistivity changes rapidly with no hysteresis observed in the imbibition/drainage cycle. At high Sw, there is another region that exhibits no hysteresis. In the mid-saturation range, hysteresis is found in the imbibition/drainage cycle. In this hysteretic region, resistivity measured during imbibition is consistently less than that measured during drainage, and reaches resis-

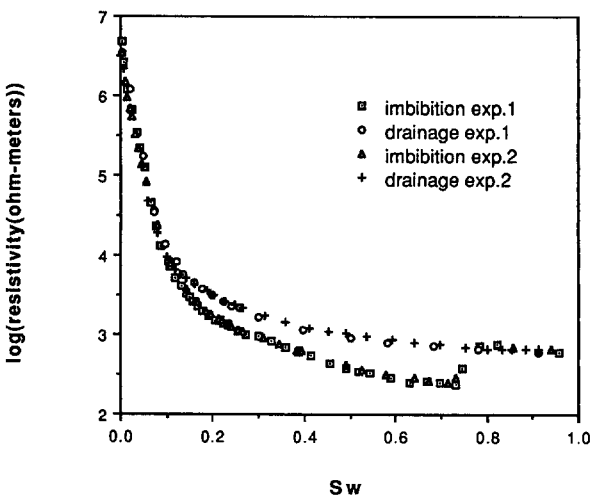

FIG. 4. Log ρ versus Sw for sample CH58-79; measurement frequency is 60 kHz. Data are from experiment 1 (exp. 1) and experiment 2 (exp. 2).

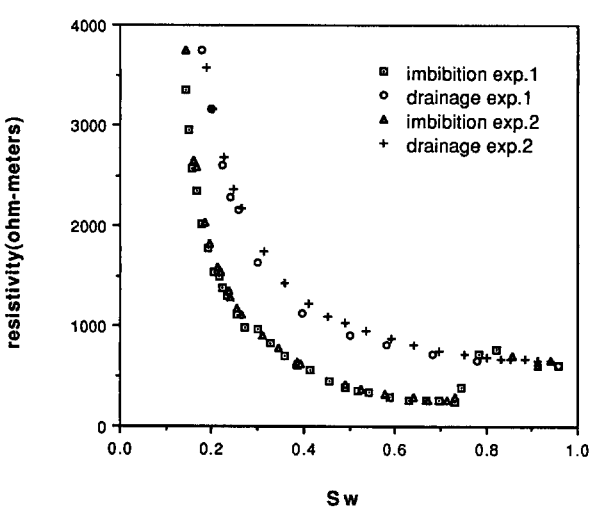

FIG. 5. Resistivity versus Sw for sample CH58-79 in regions 2 and 3; measurement frequency is 60 kHz. Data are from experiment 1 (exp. 1) and experiment 2 (exp. 2).

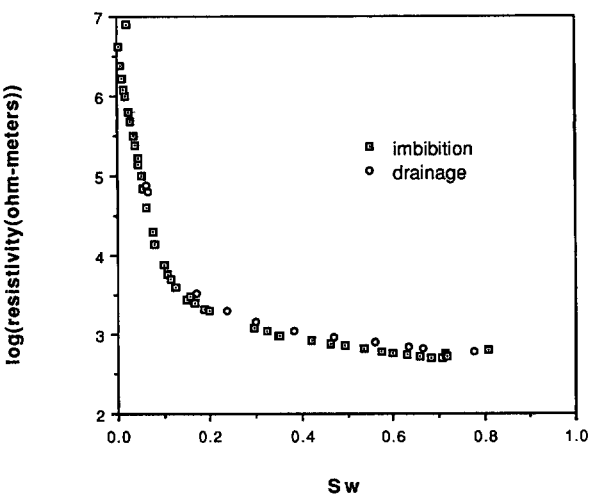

FIG. 6. Log ρ versus Sw for sample CH58-79, experiment 3; measurement frequency is 60 kHz.

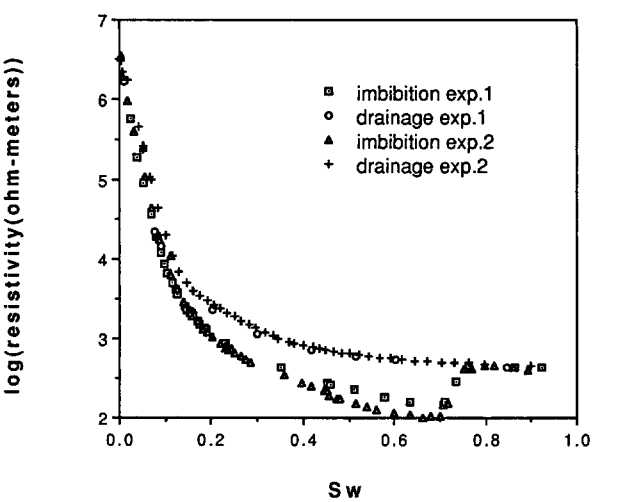

FIG. 7. Log ρ versus Sw for sample CH61-79; measurement frequency is 60 kHz. Data are from experiment 1 (exp. 1) and experiment 2 (exp. 2).

tivity values lower than that of the fully saturated rock. In general, there exists some variation in repeat experiments in the magnitude of the measured resistivity values within the hysteretic region. In one case, a repeat experiment closely reproduced earlier results; in another case the hysteresis was eliminated in the repeat experiment. All of these factors will be considered in the interpretation of the data.

INTERPRETATION

In this experimental study of the resistivity of partially saturated rocks, the two experimental variables are the level of water saturation and the saturation history. The electrical resistivity of a partially saturated sandstone sample can be related to the pore-scale volumes and geometries of three phases in the system—the rock matrix, the water, the air. During an experiment when Sw and saturation history are varied, the volume and geometry of the rock matrix will remain constant; it is the changing volumes and geometries of the air and water in the pore space that must be considered in assessing the changing resistivity of the system.

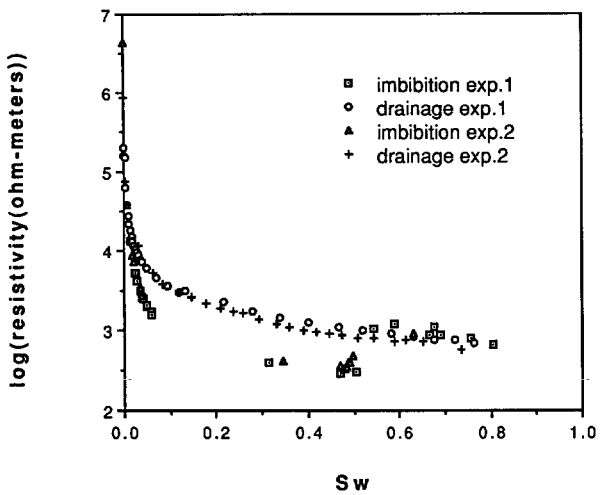

FIG. 8. Log ρ versus Sw for sample Berea 100; measurement frequency is 60 kHz. Data are from experiment 1 (exp. 1) and experiment 2 (exp. 2).

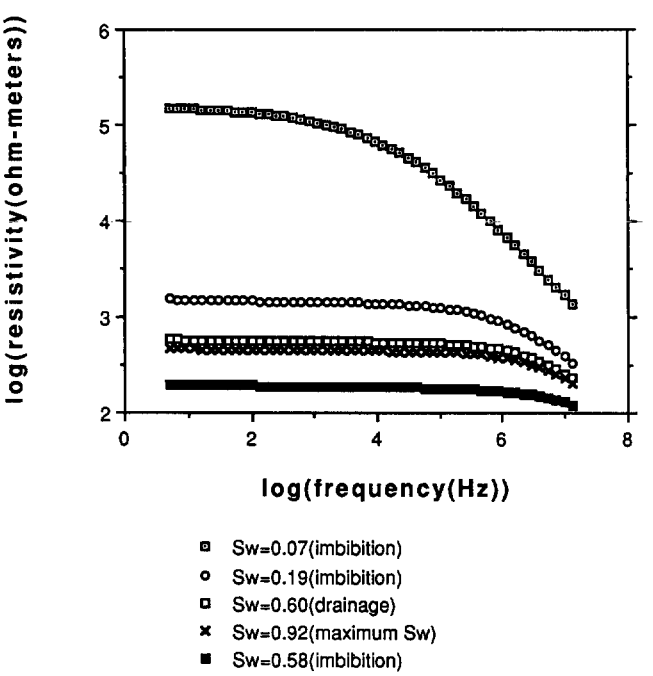

FIG. 9. Log ρ versus log frequency for sample CH61-79 at various levels of water saturation.

With the completion of this study, there now exist three data sets, collected using the same experimental procedures for varying saturation, that show saturation-related hysteresis in (1) electrical resistivity (this study), (2) dielectric constant (Knight and Nur, 1987a) and (3) elastic wave velocities (Knight and Nolen-Hoeksema, 1990). A simple model of the types of pore-scale fluid geometries that are obtained with the imbibition and drainage techniques used in these three studies was proposed by Knight and Nur (1987a) to explain the observed dielectric hysteresis. This model has since been used as the basis for theoretical modeling of the dielectric hysteresis (Endres and Knight, 1991), with excellent agreement found between theory and data. The same model has also been applied to the interpretation and theoretical modeling of the hysteresis in elastic wave velocities (Knight and Nolen-Hoeksema, 1990; Endres and Knight, 1991). This model of Knight and Nur (1987a) is summarized below then extended to the interpretation of the electrical resistivity data from this study.

Model of Imbibition and Drainage Fluid Geometries

In Figure 10 is a schematic illustration of the fluid geometries created during imbibition and drainage. The saturation process and the level of saturation determine the geometry of the air and the water in the pore space of the rock. At low levels of water saturation the water exists in the pore space as surface water, forming a thin coating on the surface of the solid component (Geometry A in Figure 10). At these low saturations, the adsorption of water during imbibition and the desorption of water during drainage are considered to be reversible with respect to geometry, i.e., the relative geometries of the rock, water, and air are the same for both processes. At higher saturations, bulk water and air occupy the central volume of the pore space. At these saturations the processes of imbibition and drainage produce very different geometries of the water and air phases. During imbibition the water tends to continue coating the pore surfaces. This creates thick, metastable surface layers of water, separated by a thin central air phase (Geometry B in Figure 10). As saturation increases, a point is reached at which this geometrical arrangement of water and air becomes unstable and a pore-scale rearrangement to a more stable state occurs, a phenomenon described by Haines (1930). This more stable geometry is envisioned as one in which the air breaks up to form spherical bubbles and the water accumulates to completely fill the narrow regions of the pore space (Geometry C in Figure 10). At the highest saturation level, large regions of the pore space can be treated as fully water-saturated (Geometry D in Figure 10), with trapped air in isolated pores such that Sw measured for the total sample is less than 1.0. During drainage, the thin air

phase and thick surface water layers are not recreated; water drains from the pores removing all but the tightly held thin layer of surface water (Geometry E in Figure 10). Thus, the primary difference between imbibition and drainage, seen by comparing Geometry B and Geometry E in Figure 10, is the resulting geometry of the gas phase; such a contrast in geometry was first suggested by Foster (1932) in a study of condensation in silica gel.

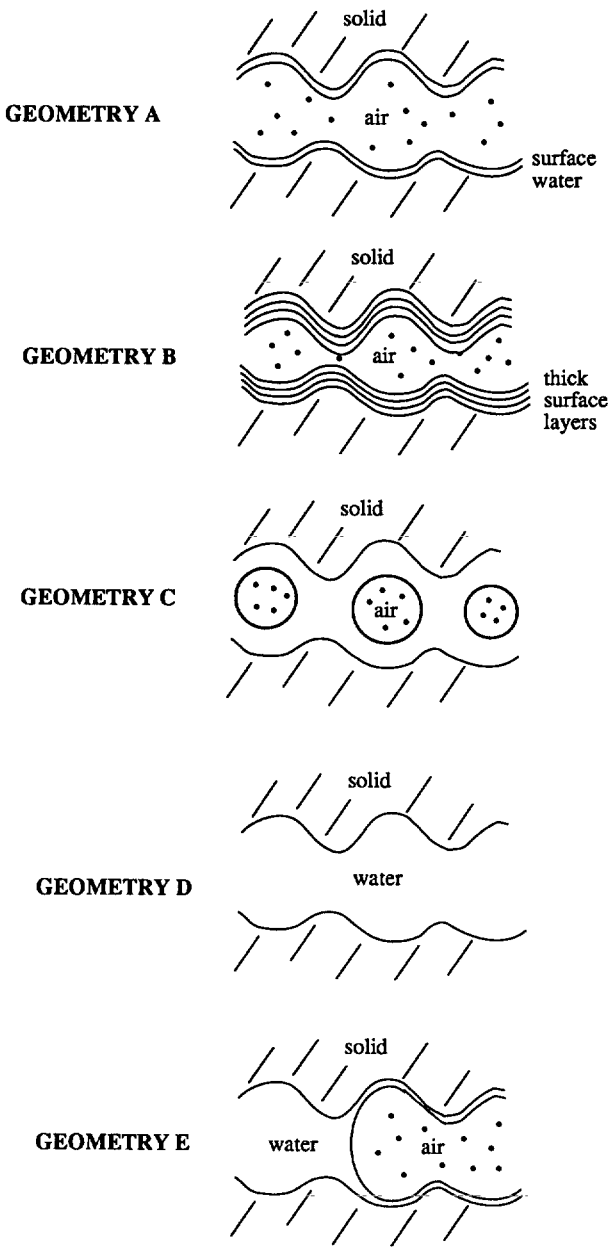

FIG. 10. Schematic illustration of the fluid geometries at various saturations during imbibition and drainage. GEOMETRY A: At low saturations a thin layer of surface water coats the solid. GEOMETRY B: Thick surface layers of water develop during imbibition. GEOMETRY C: The fluids rearrange to a more stable geometry. GEOMETRY D: Large regions of the pore space become fully water-saturated at the highest saturations. GEOMETRY E: The drainage of water from the pore space removes all but the thin layer of surface water.

Can this simple model of changing pore-scale fluid geometries explain the variation in resistivity observed in this study?

The Relationship Between Fluid Geometries and Resistivity: Region 1

Focusing first on region 1 at low Sw, it is reasonable to assume that this region corresponds to the addition and removal of surface layers of water at the solid/pore interface. The geometry at these saturations thus corresponds to Geometry A in Figure 10. It is informative to determine the thickness of the surface water in this saturation region. Assuming that the water covers the total internal surface area of a sample in uniform monolayers of water, the thickness of the surface layer, given in terms of the number of monolayers of water, can be calculated from the measured saturation level:

$$\text{number of monolayers} = \frac{S_w \phi V_T}{S t_m},$$

where ϕ is porosity, V_T is the total volume of the sample, S is the measured surface area of the sandstone (given in Table 1), t_m is the thickness of a monolayer of water; $t_m = 0.35$ nm (Thorp, 1959).

The data for CH61-79 at low Sw from experiments 1 and 2 are given as log ρ versus monolayers of water in Figure 11. It is interesting to note that ρ begins to drop as soon as Sw starts to increase from the dry state. This is in contrast to the dielectric data in which there was little change in the dielectric constant until the completion of the first monolayer (Knight and Nur, 1987b; Knight and Endres, 1990). As Sw increases, ρ continues to decrease rapidly until the completion of three to four monolayers at which point the hysteretic region begins. Very similar results were obtained for the other two samples with the lower limit of the hysteresis corresponding to the completion of three to four monolayers in both cases.

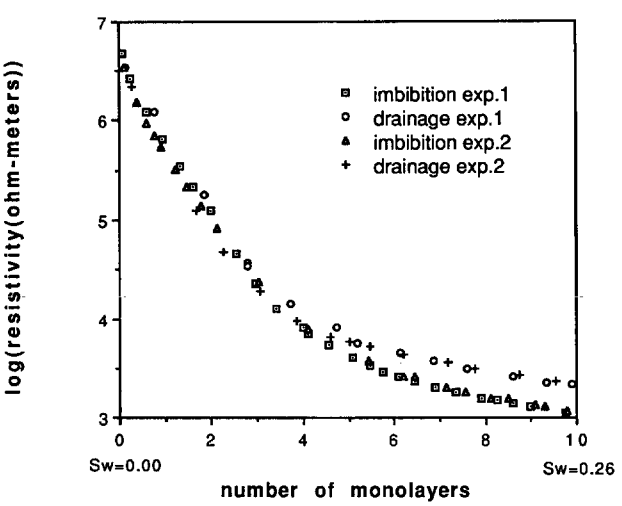

FIG. 11. Log ρ versus number of monolayers for sample CH61-79; measurement frequency is 60 kHz. Data are from experiment 1 (exp. 1) and experiment 2 (exp. 2).

The rapid decrease in ρ in region 1 can be attributed to the establishment of surface conductivity at the rock/water interface. Surface conduction in rocks has often been referred to as the "shaley sand" effect as it is most pronounced when high surface area materials, such as clays are present. The full establishment of the magnitude of such surface effects will be attained once the water coating of the surface is complete. In the unsaturated zone it is reasonable to assume that a surface layer of water will be present in all materials. In addition it is clear that saturation history will not affect the relationship between ρ and Sw at these saturations. At these low saturations it can be concluded that there exists a unique and reproduceable relationship between ρ and Sw.

The Relationship Between Fluid Geometries and Resistivity: Regions 2 and 3

In regions 2 and 3, the change in resistivity of the samples is related to the presence of water and air in the central volume of the pore space. The most commonly used expression for describing the variation of ρ with Sw at these higher saturations is Archie's relationship in which ρ is proportional to Sw^{-n}, where n is referred to as the saturation exponent (Archie, 1942). It is becoming increasingly apparent that the variation in ρ with Sw is more complex than can be described by this relationship. In particular there are an increasing number of examples in which a variation in n with Sw has been observed. This variation in n has been attributed to the order of saturation or desaturation of pores or pore networks (Longeron et al., 1989; Argaud, 1990); i.e., the variation in Sw in individual pores is as important in determining the resistivity behavior as the macroscopic Sw for the entire porous sample. The specific form of variation in ρ observed in the saturation region 2 in this study can also be explained in terms of such pore-scale effects.

Six of the seven data sets presented show the same form of dependence of ρ on Sw in the hysteretic region. There are three important features of the data that need addressing:

1) Throughout the entire hysteretic region, for the same Sw, ρ measured during imbibition is less than ρ measured during drainage.
2) The imbibition ρ throughout much of the hysteretic region reaches values less than the ρ of the fully saturated sample.
3) A critical phenomenon is present in the imbibition data where a small increase in saturation causes ρ to increase rapidly to join the drainage curve.

It will be assumed, as proposed in the model of Knight and Nur (1987b), that the imbibition process used in this experiment favors the establishment of thick surface layers of water and a thin interconnected gas phase. This corresponds to Geometry B in Figure 10. At the low saturation end of the hysteresis loop, where the drainage and imbibition data first start to diverge, it can be argued that the surface distribution of water obtained with imbibition is more favorable for electrical conduction through the pore water than the water distribution obtained during drainage. Considering conduction through the water alone, however, cannot explain the occurrence of resistivities during imbibition in a partially saturated rock that are less than the resistivity of the fully saturated rock. An additional parameter must be considered. I propose the idea that there exists surface conduction at the air/water interface that must be included when considering conduction in partially saturated rocks.

While much attention has been given to the surface conduction at the rock/water interface, there has been no previous consideration of the possiblity of surface conduction at the air/water interface in partially saturated rock samples. There are, however, a number of references to the magnitude of the charge density and zeta potential at the air/water interface, measured on bubbles in aqueous solutions (Alty, 1924; McShea and Callaghan, 1983; Laskowski et al., 1989), that suggest that the surface condition at this interface can be of the same magnitude as surface conduction at the rock/water interface. As with surface conduction at the rock/water interface, it is to be expected that if the bulk water in the central volume of the pore space is highly conductive the surface conduction at the air/water interface will make a relatively small contribution to the total conductivity. The use of deionized water in this study has therefore most likely enhanced this effect.

The imbibition geometry results in a large continuous surface area for the air/water interface—much larger than exists with the drainage geometery. It is this aspect of the imbibition process that is interpreted as being responsible for the ρ values measured during imbibition that are less than the ρ of the fully saturated rock. During imbibition, there is a contribution to the conductivity of the system from both the water and the air/water interface. When the imbibition geometry reaches the critical saturation point, the fluids rearrange; the air phase becomes disconnected and the size and connectivity of the air/water interface is reduced. The reduction in the size and connectivity of the interface causes a corresponding reduction in the magnitude of the surface conduction at the air/water interface; thus the rearrangement of fluids on the pore scale is observed as a jump in resistivity on the macroscopic scale. This corresponds to the sudden "collapse" in the hysteresis loop observed in the data at a saturation of approximately 0.7 for CH58-79 and CH61-79 and at a saturation of approximately 0.5 for Berea 100.

The drainage data show a much simpler dependence of ρ on Sw. This is attributed to the fact that an extended gas phase and the associated surface conduction at the air/water interface are not established. The drainage geometry favors the segregation of pore fluids such that regions of the pore space tend to be either fully water-saturated or fully air-saturated. At Sw values above the critical point, in region 3, the imbibition data match the drainage data because the drainage geometry dominates the system after the rearrangement of the pore fluids.

Hysteresis clearly exists in electrical resistivity data at intermediate levels of water saturation. The cause of the hysteresis is interpreted to be the changes in pore-scale fluid distribution associated with the saturation history. In assessing the relevance of these results to studies of the unsaturated zone, it is important to consider the reproduceability and stability of these effects.

SATURATION-RELATED HYSTERESIS

The form of the hysteresis and the results of repeat experiments provide information about the fundamental nature and the stability of the saturation-related hysteresis. In this study it has been concluded that different saturation processes produce different "types" of fluid geometries that, in turn, lead to corresponding and distinctive resistivity versus water content curves. The reproduceability and stability of the observed hysteresis during an imbibition/drainage cycle is thus controlled by the reproduceability and stability of the fluid distributions that occur during changes in saturation.

The experimental data have shown, in general, repeating a saturation process produces qualitatively the same form of resistivity response. The imbibition/drainage data for the three samples are strikingly similar in functional form. Each time a sample is saturated however, even though the gross features of the fluid geometries can be reproduced, it is unlikely that all details of the pore-scale fluid distribution will be reproduced; i.e., the water will not occupy the exact same locations in subsequent experiments. As a result, there can be some variation in the absolute values of measured resistivity within the hysteresis loop. In repeat experiments a wide range of behavior was observed from close reproduction of the hysteresis loop to elimination of the hysteresis. The elimination of hysteresis suggests that, in this case, the water during imbibition assumed a drainage type of geometry. It is clear that the reproduceability of the hysteresis depends on the reproduceability of the saturating process.

In a similar way, the stability of the hysteresis depends on the stability of the fluid distributions. This is an important consideration in applying the results of this study to in-situ measurements. One test was carried out to directly test the stability of the fluid distributions. During experiment 2 for CH61-79 (data shown in Figure 7), the experiment was interrupted at $Sw = 0.43$ during imbibition and at $Sw = 0.51$ during drainage and the sample wrapped in plastic wrap to keep Sw constant for a period of two months. After the two months, there was no change in resistivity for either the imbibition or drainage case. This indicates that both the imbibition and drainage geometries in this experiment were stable on the time scale of two months.

In this one direct test of the stability of the fluid distributions there was no difference indicated between the stability of the imbibition and drainage states. Other evidence, however, suggests that imbibition tends to produce a less stable fluid distribution. Based on the proposed geometrical models, the imbibition geometry with the large water/air interface has a much higher interfacial free energy, making it less stable from a simplified thermodynamic perspective. The observation that the imbibition curve "collapses" to join the drainage curve at high saturations suggests rearrangement at this point to a lower energy, more stable state.

The experimental data from this study suggest a high level of reproduceability and stability of the hysteretic region, for the conditions and time scale of the laboratory study. An obvious extension of this study is to asssess the effect of in situ conditions, longer time scales, and a more complicated saturation history on the resistivity response.

CONCLUSIONS

The results of this study clearly indicate that measured values of electrical resistivity can depend on the saturation history of the sample. With the saturation techniques used in these experiments, imbibition and drainage each tended to produce a characteristic dependence of resistivity on saturation. The reproduceability and the stability of the hysteresis loop are closely linked to the reproduceability and stability of the fluid distributions.

In the unsaturated zone of the subsurface, naturally occurring saturation processes such as infiltration and evaporation will undoubtedly lead to differences in the pore-scale distribution of water and air. As seen in the results in this study, it is expected that each of these natural saturation processes will have a corresponding characteristic resistivity response. This implies that there will not be a simple relationship between measured resistivity and in-situ water content, as the relationship between these two parameters depends on saturation history. In the interpretation of resistivity data from a specific region of the unsaturated zone, it becomes essential that the effect of saturation history on the resistivity-Sw relationship for that region be determined. Results from other laboratory studies of the dielectric constant (Knight and Nur, 1987a) and elastic wave velocities (Knight and Nolen-Hoeksema, 1990) suggest that this is a necessary first step in the interpretation of any geophysical data from the unsaturated zone.

The effect of saturation history on geophysical data sets undoubtedly complicates the extraction of water content from geophysical measurements. The existence of this effect, however, suggests that geophysical data could be used to recover additional information. Once the link between natural saturation processes and the corresponding geophysical response can be determined, it may be possible to use geophysical data sets to obtain information about saturation history and fluid distribution, parameters that are very important in characterizing transport in the unsaturated zone.

ACKNOWLEDGMENTS

This research was supported by the Natural Sciences and Engineering Research Council of Canada. I would like to thank Ana Abad for assistance in the laboratory, and the Rock Physics Group at the University of British Columbia for numerous helpful, and enjoyable, discussions.

REFERENCES

Alty, T., 1924, The cataphoresis of gas bubbles in water: Proc. Roy. Soc. London Ser. A, **106**, 315–340.

Archie, G. E., 1942, The electrical resistivity log as an aid in determining some reservoir characteristics: Am. Inst. Min., Metalurg., Petr. Eng., **146**, 54–67.

Argaud, M., 1990, Rock heterogeneity: key for explaining non-linear resistivity index curves: Transactions Soc. Prof. Well Log Analysts 31st Ann. Log. Sym.

Bourbie, T., and Zinszner, B., 1984, Saturation methods and attenuation versus saturation relations in Fontainebleu sandstone: 54th Ann. Internat. Mtg., Soc. Expl. Geophys., Expanded Abstracts, (Page) 344–350.

Brunauer, S., Emmett, P. H., and Teller, E., 1938, Adsorption of gases in multimolecular layers: J. Am. Chem. Soc., **60**, 309–319.

Endres, A. L., and Knight, R. J., 1991, The effects of pore scale fluid distribution on the physical properties of partially saturated tight sandstones: J. Appl. Phys., **69**, 1091–1098.

Foster, A. G., 1932, The sorption of condensible vapours by porous solids. Part I. The applicability of the capillary theory: Trans. Farady Soc., **28**, 645–657.
Haines, W. B., 1930, Studies in the physical properties of soil. V. The hysteresis effect in capillary properties and the modes of moisture distribution associated therewith: J. Agric. Sci., **20**, 97–116.
Knight, R. J., 1985, The dielectric constant of sandstones, 5 Hz to 13 MHz: Ph. D. dissertation, Stanford University.
Knight, R. J., and Enders, A. L., 1990, A new concept in modeling the dielectric response of sandstones: Defining a wetted rock and bulk water system: Geophysics, **55**, 586–594.
Knight, R. J., and Nolen-Hoeksema, R., 1990, A laboratory study of the dependence of elastic wave velocities on pore scale fluid distribution: Geophys. Res. Lett., **17**, 1529–1532.
Knight, R. J., and Nur, A., 1987a, Geometrical effects in the dielectric response of partially saturated sandstones: The Log Anal., **28**, 513–519.
Knight, R. J., and Nur, A., 1987b, The dielectric constant of sandstones, 50 kHz to 4 MHz: Geophysics, **52**, 644–654.
Laskowski, J. S., Yordan, J. L., and Yoon, R. H., 1989, Electrokinetic potential of microbubbles generated in aqueous solutions of weak electrolyte type surfactants: Langmuir, **5**, 373–376.
Longeron, D. G., Argaud, M. J., and Feraud, J. P., 1989, Effect of overburden pressure and the nature and microscopic distribution of fluids on electrical properties of rock samples: SPE Format. Eval., **4**, 194–202.
McShea, J. A., and Callaghan, I. C., 1983, Electrokinetic potentials at the gas-aqueous interface by spinning cylinder electrophoresis: Colloid Polym. Sci., **261**, 757–766.
Thorp, J. M., 1959, The dielectric behavior of vapours adsorbed on porous solids: Trans. Faraday Society, **55**, 442–454.